Supplementary information

1. Fitting the second-order reaction rate constant *k*

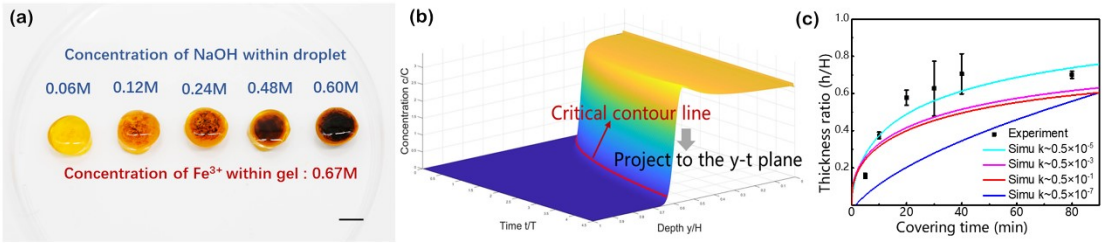

Fig. S1. Detailed process of fitting the second-order reaction rate constant *k*. (a) Titration experiment to determine the critical concentration for Fe_3O_4 nanoparticles to precipitated out of the solvent environment. Scale bar: 5mm. (b) Using the critical concentration of Fe_3O_4 to approximate the critical contour line, whose projection on the y-t plane represents the position of the reaction front versus covering time. (c) Utilizing the projection of critical contour line and the experimental data of thickness ratio to fit the parameter *k*.

Fig. S1 illustrates the detailed process of fitting second-order reaction rate constant *k* in our study. The solid product of precipitation reaction is assumed to precipitate from the solvent above a critical concentration. We employ a titration experiment to estimate such a critical concentration. As shown in Fig. S1-a, PAAm hydrogels with 0.67M Fe^{3+} ions (and 0.33M Fe^{2+} ions) are dip-dyed by droplets containing 0.06~0.60M OH^- ions. After 10 seconds, we find that the iron ions inside the hydrogel can be precipitated into black product when the concentration of OH^- ions in the droplet is above 0.24M. Since the iron ions are excess, the critical

concentration of Fe_3O_4 nanoparticles is determined by the concentration of OH^- ions, and is about 0.03M according to the reaction formula (1). Fig. S1-b shows a 3D curved surface illustrating the profile of Fe_3O_4 concentration versus the covering time and the depth in the 1D ion transfer printing process. It is seen that the concentration of Fe_3O_4 nanoparticles is high near the surface of the hydrogel (yellow area), while is low at the bottom of the hydrogel (blue area). The sharp transition between the two areas also implies the existence of the reaction front. As determined by the titration experiment, the critical concentration of Fe_3O_4 nanoparticles to be visible is about 0.03M. Thus, we can cut the curved surface with a horizontal plane with a height of 0.03 M, and then project the intersecting line onto the plane of depth versus time. The intersecting line is denoted as the critical contour line (red line) in Fig. S1-b. The projection of this line represents the location of the reaction front versus covering time, which is also viewed as the thickness of the magnetic zone. Fig. S1-c shows the critical contour line fitted by different values of *k*. It is seen that the optical value k~0.5×10^{-5} $m^3mol^{-1}s^{-1}$ can fit the experimental data well and it is used in the following simulation.

2. Calculation of specific absorption rate (SAR)

SAR of magnetic nanoparticles inside the patterned magnetic hydrogel has been determined in following steps. Here the magnetic hydrogel is fabricated with 0.67M Fe^{3+}, 6M OH^- and heated by specific AMF (current=300A, frequency = 230 kHz). Firstly, two material constants C_s and C_g are approximated by the specific heat capacity of magnetite and water as C_s=0.625J/$(g\cdot K)$, C_g = 4.186J/$(g\cdot K)$. According to the literature [1], the percentage of Fe_3O_4 in the product of precipitation reaction after

60min is about 35.6%, which gives $\eta \sim 0.3$. Secondly, the mass fraction f_m of Fe_3O_4 in the magnetic zone could be approximated by the simulation result. The result of 1D reaction-diffusion model reveals a uniform concentration of Fe_3O_4, i.e. 0.33M. For pure Fe_3O_4, we could define its dense concentration as the density divided by molar weight i.e. $c_d \cong \rho_{\mathrm{m}} / M_{\mathrm{m}}$, where ρ_{m} is the density of Fe_3O_4, and M_{m} is the molar weight. When Fe_3O_4 is mixed with hydrogels by a specific volume fraction f_v, and it has a prescribed concentration c. Then the volume fraction of Fe_3O_4 could be approximated by $f_v = c / c_d$ in the mixture. For pure Fe_3O_4, its dense concentration is about $c_d = 22.33M$. Hence, the volume fraction of Fe_3O_4 in the magnetic zone could be calculated as f_v=1.48% (~0.33/22.33) in our case. The volume fraction could be converted into the mass fraction $f_m = \rho_m f_v / \left[\rho_m f_v + \rho_g \left(1 - f_v\right) \right]$, where ρ_g is the density of the hydrogel. Plugging $f_v = 1.48\%, \rho_m = 5.17 g/cm^3, \rho_g = 1.0 g/cm^3$ we can obtain $f_m = 7.3\%$. This result is comparable to our previous study [2], where the mass fraction of Fe_3O_4 nanoparticles is 2.83% in the magnetic hydrogel prepared by in-situ precipitation method with 0.2M Fe^{3+}. Thirdly, the initial slope $\Delta T / \Delta t$ is determined experimentally. As shown in Figure 4i, we take $\Delta T / \Delta t = 0.6 K/s$ under the following condition (0.67M Fe^{3+}, 6M OH^-, 60min covering time). Finally, plugging $\eta, f_m, C_s, C_g, \Delta T / \Delta t$ into equation (8), we can obtain SAR as 107.6W/g.

3. Configuration of 1D reaction-diffusion model

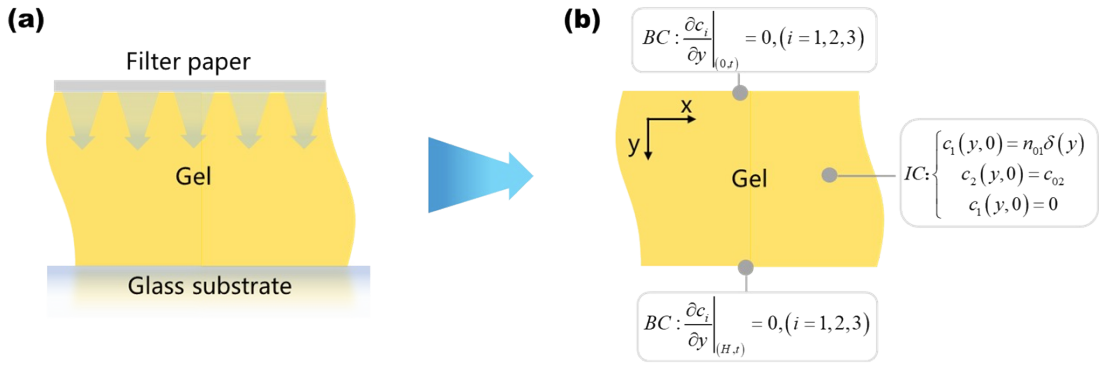

Fig. S2. Schematic of initial and boundary conditions of 1D reaction-diffusion model. Schematic of experimental implementation (a), and corresponding configuration of initial conditions (IC) and boundary conditions (BC) (b).

4. Microstructure characterization of patterned magnetic hydrogel

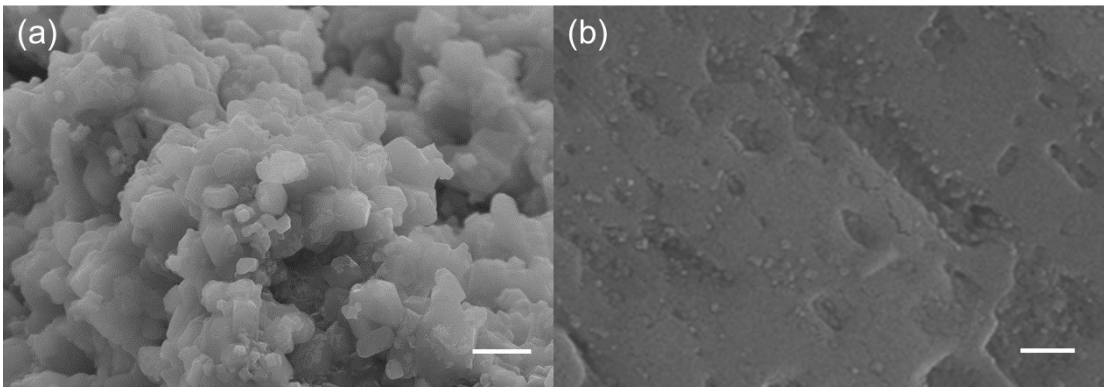

Fig. S3. SEM images of freeze-dried hydrogel with magnetic patterns. (a) Magnetic nanoparticles near the surface of hydrogel, scale bar: 1μm. (b) Magnetic nanoparticles in the central part of the hydrogel matrix, scale bar: 500 nm.

We fabricated a specimen with 0.67M Fe^{3+}, 6M OH^- and 90min covering time. The specimen was first freeze-dried and then was coated with platinum powder. After that, a scanning electron microscopy (XL Series-30, Philips, USA) was used to characterize the side plane of hydrogel with magnetic pattern. As shown in Fig.S4-a, the size of precipitated magnetic nanoparticles near the surface of the hydrogel ranges

from 200~1000 nm. Fig.S4-b shows that as the diffusing depth increases, the precipitated magnetic nanoparticles possess smaller size in the hydrogel matrix, ranging from 50~100nm.

References

1. H. Rashid, M. A. Mansoor, B. Haider, R. Nasir, S. B. Abd Hamid and A. Abdulrahman, *Separation Science and Technology*, 2019, **55**, 1207-1215.
2. J. Tang, Q. Yin, Y. Qiao and T. Wang, *ACS Appl Mater Interfaces*, 2019, **11**, 21194-21200.